

# PROGRESS FOR STABLE ARTIFICIAL LIGHTS DISTRIBUTION EXTRVCTION ACCURACY AND ESTIMATION OF ELECTRIC] POWER CONSUMPTION BY MEANS OF DMSP/OLS NIGHTTIME IMAGERY

MASANAO HARA<sup>1-2</sup>, SHUHEI OKADA<sup>1</sup>, HIROSI YAGI<sup>1</sup>, TAKASHI MORIYAMA<sup>3</sup>,  
KOJI SHIGEHARA<sup>1</sup> AND YASUHIRO SUGIMORI<sup>4</sup>

## Abstract

The Noise Reduction Filter (NRF) that is developed by the authors is applied to extract artificial nightlight components of a time series DMSP/OLS-VIS dataset. High frequency components from the time series DMSP/OLS-VIS dataset are exhausted and a direct current component is extracted by the NRF that is one of the Fourier analysis techniques. The inference of cloud and other disturbance noise are also removed, and a stable artificial nightlight is extracted by the NRF filtration.

The intensity value in high power light areas observed by DMSP/OLS-VIS is saturated because of narrow dynamic range of the sensor gain. A simple model called "Deltaic Model" developed by authors corrected those saturated value. Verification of the accuracy of correction methods above described is carried out by comparison with electric power consumption of the calculated values from the model and statistical ones of each prefecture in Japan. Correlation of the values is satisfactory as shown  $R^2 = 0.725$ .

The results of this work shows the remote sensing method by using the DMSP/OLS-VIS nighttime imagery with the correction methods above described is useful to estimate the electric power consumption through a year of fixed areas.

*Keyword: DMSP/OLS-VIS, NRF filtration, Deltaic Model*

## I. Introduction

Since humans first discovered fire in prehistoric times, they have sought to improve the quality of life through use of energy. Beginning with the Industrial Revolution in the 18<sup>th</sup> Century, human activity of this sort has increased rapidly. From Edison's invention of the electric light bulb in the 19<sup>th</sup> Century to "the Information Superhighway" of today, electricity has made possible the comfortable human lives we enjoy today.

Nowadays, energy consumption level, par-

ticularly electric consumption level in a given area is the barometer of human activity there. From this, it can be derived things such as mobility, economic activity, and population of the country or its area. Therefore, if the electric power consumption of an area is known, it can be also estimated the degree of such human activity there. Such activity consumes electric power in large quantities, and increases fuel consumption used to generate electric power, especially consumption of a fossil fuel. Electric power consumption is one

1 VTI Research Institute, VisionTech Inc.

2 Disaster Prevention Research Group, National Research Institute for Earth Science and Disaster Prevention

3 Satellite Program and planning department office of satellite technology, research and applications, National Space Development Agency of Japan.

4 Center for Environmental Remote Sensing, Chiba University.

of the key indicators to predict global environment changes, because it is believed that mass consumption of a fossil fuel may seriously influence phenomenon such as global warming (JMA, 1984, IPCC, 1990).

Elvidge et al. (2001) observed the distribution of artificial light using the Operational Linescan System (OLS) of the U.S. Defense Meteorological Satellite Programmed (DMSP) and has reported that there is a certain relation between the distribution area and electric power consumption. Moreover, Elvidge et al. (1997a, 1997b and 1997c, 1999, and 2001), Doll et al. (2000), Nakayama, Tanaka (1983), and Nakayama (1993) have published research, which shows a relationship between human social activity related to electric power consumption and distribution of intensity of artificial nightlight.

The satellite features two channels, a visible near infrared sensor (VIS) and a thermal infrared sensor (TIR) in DMSP/OLS; the DMSP/OLS-VIS can observe the distribution of lights by controlling its gain and level at night time. If artificial nightlight areas can be extracted accurately from DMSP/OLS-VIS observation data, it might be possible to improve accuracy of parameters for estimating power consumption. For that purpose, it is necessary to solve the following four problems:

- 1) Influence of clouds
- 2) Change of the standard by gain control of an DMSP/OSL-VIS sensor
- 3) Random noise generated by a certain factor
- 4) Saturation of DN value of the DMSP/OLS-VIS sensor

In this research, the method of improving the accuracy of artificial nightlight extraction and for removing irregularities noise is developed by the authors (2003a and 2003b) using a Noise Reduction Filter (NRF). Evaluation of the NRF Method is carried out to compare the image created with the one processed by the Elvidge Method (2001) as well as the Land Use Data (LUD) of Digital Land Information Data prepared by the Geographical Survey Institute (GSI). Furthermore, a method to estimate electric power consumption

from the artificial nightlight dataset is developed. The values of electric power consumption, reduced by saturation due to sensor gain, are corrected and improved by using the simple model of distribution and intensity of artificial nightlight. Verification of the accuracy of the above-mentioned correction is carried out by comparison of electric power consumption between the calculated values from the extracted artificial nightlight intensity and the statistical values (FEPC, 2002) of each prefecture in Japan.

## II. Data Used in Analysis

### 2.1. DMSP/OLS Data

The DMSP satellite orbits the earth at an altitude of 830km about every 101 minutes. DMSP/OLS-VIS and DMSP/OLS-TIR observe each place twice a day with about 3000km observation swath. The specifications of DMSP are shown in Table 1. The observed data are sent to National Geophysical Data Center (NGDC, USA), and they are being distributed from NGDC to the user. Three DMSP satellites named F13, F14 and F15 are currently deployed.

DMSP carries seven sensors. The main purpose of its OLS sensors is to monitor cloud distribution and cloud-top temperature. The specifications of OLS are shown in Table 2. An observation wavelength range of OLS-VIS is 0.4-1.1 $\mu$ m in daytime, and 0.47-0.95 $\mu$ m in nighttime. Its observation resolution is 6 bits per pixel, and the value of the image data is shown by the relative Digital Number value

Table 1. Specifications of DMSP satellite.

| Orbit    | Sun-Synchronnous near-polar orbit   |
|----------|---|
| Altitude | 830 km  |
| Term     | 101 minuts  |
| Sensor   | OLS (Operational Linescan System)<br>SSM/1 (Microwave Imager)<br>SSMT/2 (Atmospheric Water Vapor Profiler)<br>SSJ/4 (Precipitating Electron and Ion Spectrometer)<br>SSM/T (Atmospheric Temperature Profiler)<br>SSIES (Ion Scintillation Moitor)<br>SSM (Magnetometer) |

(DN value) of 0 - 63. The sensor gain and the level of OLS-VIS are controlled during night orbit. The first purpose of doing this is to generate homogeneous cloud images without moonlight influence in any sweep angle of the sensor, so that weather specialists of the U.S. Air Force may observe them. By the controlling of gains and levels of the sensor makes light saturation sometimes in the place where the high optical intensity such as a large urban area, however, to the contrary, forest fires, fishing boat lights, artificial light in urban areas and so on can be possibly detected. An observation wavelength range of OLS-TIR is 10.0-13.4 $\mu$ m. Its pixel resolution is 8 bits at the range of 190K-310K (K=Kelvin) and a DN value is shown by the equal division value of 0-255.

OLS-VIS and OLS-TIR data has two types of observation modes, fine mode and smooth mode. The spatial resolution of the fine mode is 0.55kmx0.55km per pixel, and the smooth mode is 2.7kmx2.7km per pixel. The value

of smooth mode is the mean value of 5pixelsx5pixels of fine mode. NGDC also offers re-mapped OLS-VIS and OLS-TIR data with 1km x 1 km spatial resolution by using the Elvidge Method (1999) for general public distribution.

DMSP can be downloaded from the Agriculture, Forestry and Fisheries Satellite Image Database System (SIDaB) of the Ministry of Agriculture, Forestry and Fisheries Agriculture Information Resources System (AGROPEDI; <http://rmsl.agerch.argoedia.afrc.go.jp/menuJa.html>). DMSP data is transmitted from NGDC to SIDaB and it constitutes a part of SIDaB database. In this paper, both OLS-VIS and OLS-TIR of DMSP-F14 data that are downloaded from SIDaB via an Internet are used. Downloaded data is a whole year data observed by F-14, and the coverage area is a whole Japan and parts of East Asia. DN value has been converted into the 0-239 range from 0-63 in SIDaB. Fig. 1 shows the study area.

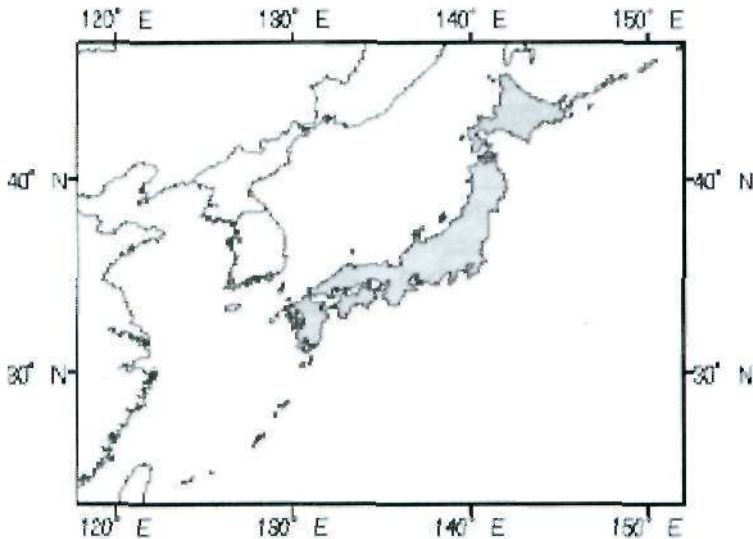


Fig.1. Outline of the study area.

Table 2. Specifications of OLS sensor.

| Band            | Wavelength        | Spatial Resolution |        | Swath  | Digitization |
|-----------------|-------------------|--------------------|--------|--------|--------------|
|                 |                   | Fine               | Smooth |        |              |
| Visible (day)   | 0.40-1. In m      | 0.55 km            | 2.7 km | 300 km | 6 bit        |
| Visible (night) | 0.47-0.95". m     | 0.55 km            | 2.7 km | 300 km | 6 bit        |
| Infrared        | 10.0-13.4 $\mu$ m | 0.55 km            | 2.7 km | 300 km | 6 bit        |

## 2.2. Digital National Land Information

Mesh data of LUD (L03-09M) of 1999 is downloaded from the Digital Land Information Data Downloading Service (<http://www.nla.go.jp/ksj/>) and used as the data for verification. This LUD mesh data are generated based on LANDSAT/TM imagery. The occupancy area of 11 kinds of land covering, such as a field, a forest, and a building lot, is recorded per mesh for longitude 45-second x latitude 30 seconds. Regarding "the building lot", the LUD is classified into five classes by using ratio of the occupancy area of each pixel according to the Jenks classification method (Minami, 2001), and created a color-mapped image using ESRI's ArcView 8.3 GIS software.

## III. Methodology

### 3.1 Elvidge Method

The extraction of urban areas detected by the artificial nightlight is carried out with the NRF Method and with the Elvidge Method (2001). In the Elvidge Method distinguishes high frequency light, that is, only artificial nightlight, and low frequency of appearance is defined as a random noise. This technique is used in many subsequent researches and this paper also chooses it to compare with the NRF Method.

The flow chart of the Elvidge Method algorithm is shown in Fig.2. The 65 scenes observed from the mid-moon to the new moon during the year 1999 are chosen, so that radiation from the moon is low and does not overly affect the image. Cloud cover conditions in selected 65 OLS-TIR images are confirmed by visual observation, and mask images at the area of cloud coverage of each 65 images are made. The OLS-VIS image, which corresponds by that mask image, is processed, and clouds are removed.

The next step, a DN threshold value of 50 (corresponding to NGDC data value 13) is established to remove clouds from the OLS-VIS image, and the appearance frequency for each pixel with a DN value of more than 50 is examined. The frequency of appearance shall carry out mask-off of 10% or less of the pixel of the number of images, and there shall

be no light. Finally, about the pixel turn on mask area, the image is reconstructed by averaging of DN value for each pixel, and it is defined as the city region image extracted by artificial light.

### 3.2. NRF Method

An NRF filter is used to attempt the extraction of artificial nightlight from the periodic function of each pixel. In other words, if there is no cloud coverage or noise in the artificial light of the urban area, the filter detects radiance from stable light, and represents the artificial lights extracting as the direct current element that is the constant term of the periodic function of each pixel.

#### 3.2.1. Pre-processing

Pre-processing is divided into two steps. The first step in pre-processing is to define the cloud area using the pair of OLS-VIS and OLS-TIR data that observed in 1999. The cloud area in an observed image is determined by comparing the temperature of suspected cloud cover with that of earth and sea, and then confirmed by visual observation. From here, the threshold for cloud cover is established, and a mask image is made from the OLS-TIR image. Next, a cloud-free image is made to combine the OLS-VIS image and the mask image. The second step in pre-processing is to generate a time series of image that consists of 36. Each image of the series is created every ten days by the method of Maximum Value Time Composition (10-day MVC) using the cloud-free images of OLS-VIS that is generated in the 1st phase.

A 10-dayMVC-VIS is a method to substitute for value of the one of a higher DN value by comparing with the DN value of each pixel for 10 days time series images. This 10dayMVC-VIS image becomes the image composed of pixel that has the strongest optical radiation (DN value) in that 10days.

#### 3.2.2. NRF Processing

The flow chart of NRF processing is shown in Fig.3. Using an LMF (Local Maximum Flitting; Sawada, 2000; Sawada, and 2001) algorithm, parameters are developed for

a cloud removal filter to extract the information from the areas that changes greatly in a short time such as NDVI of the farming area from the time series data. The filter offers the following benefits:

- 1) Improvement in fitting accuracy
- 2) Improvement in distinguishing abnormal value
- 3) Improvement in calculating local maximum value

The outline of the NRF processing is explained in the following:

$$f_t = c_0 + c_1 t + \sum_{k=1}^N \left\{ c_{2k} \sin\left(\frac{2\pi k}{M} t\right) + c_{2k+1} \cos\left(\frac{2\pi k}{M} t\right) \right\} \quad (1)$$

First, fitting of the coefficient  $C_n$  of equation (1) is done by the Least Square Fitting method, and pixel value is estimated.

Where  $C_0$ ,  $C_1$ ,  $C_{2k}$  and  $C_{2k+1}$  are the coefficient of each function;  $k$  is the frequency 1, 2, 3, 4, 6, and 12;  $N$  is the number of data; and  $M$  is the cycle. To estimate a function, it becomes a precondition that data used should be comparatively and continuously. It

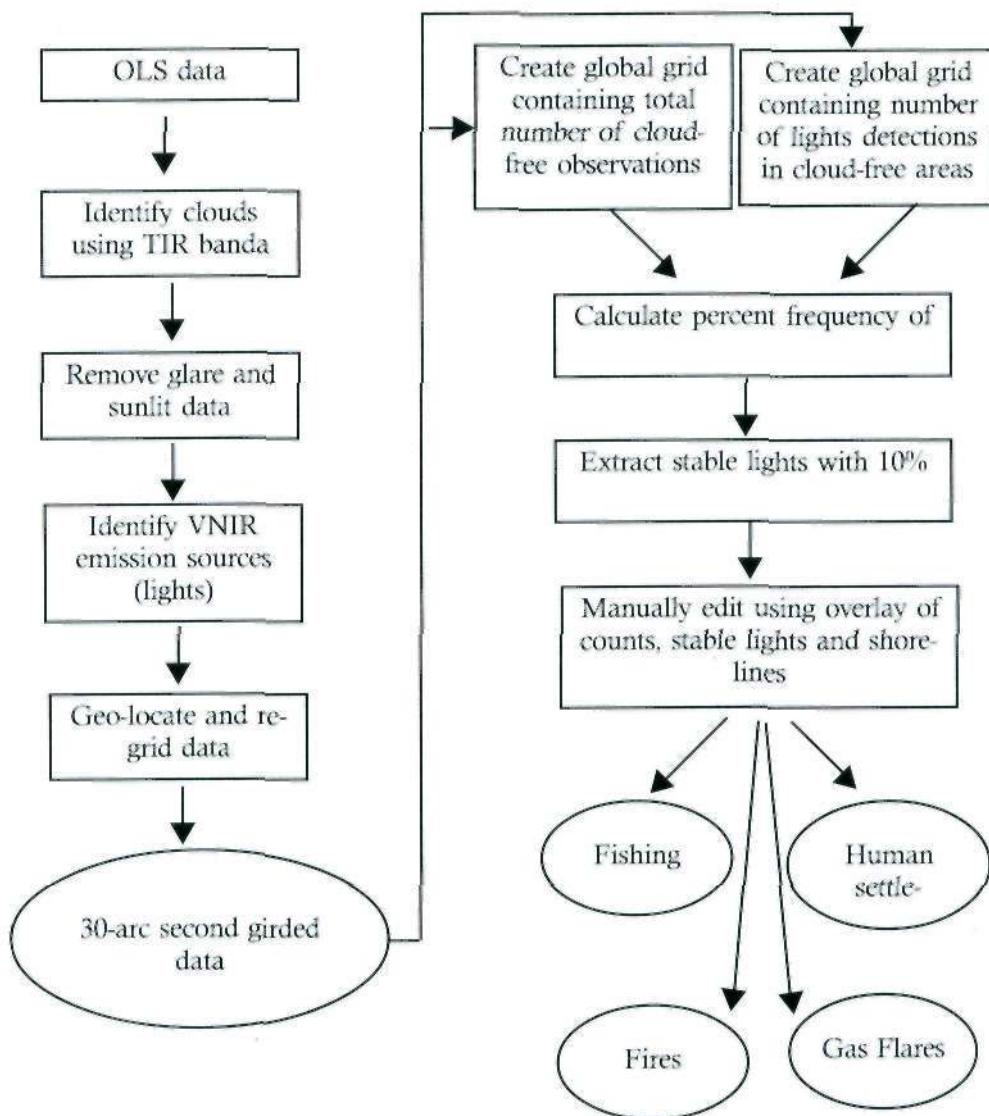


Fig.2. Flowchart of the algorithm by the Elvidge Method.

is difficult to reproduce an actual profile with a dataset the loss of data due to cloud continues. The dataset used in this research work has been ridded of clouds by using IODayMVC-VIS to a certain extent, so the continuity of the dataset is improved.

Next, cloud interference during the time series is ridded by the filter, which extracts the local maximum value as shown in Equation (2).

$$d_t = \text{Min} \left[ \text{Max} (d_{t-w+1}, d_{t-w+2}, \dots, d_t), \text{Max} (d_t, d_{t+1}, \dots, d_{t+w-1}) \right] \quad (2)$$

Where  $d_t$  is the IODayMVC-VIS; and  $w$  is the number of data to refer and was set to three in this study. So, a pixel is chosen from each of the continuous three images that are just before the criterion time image in a time series image. Also, a pixel in each continu-

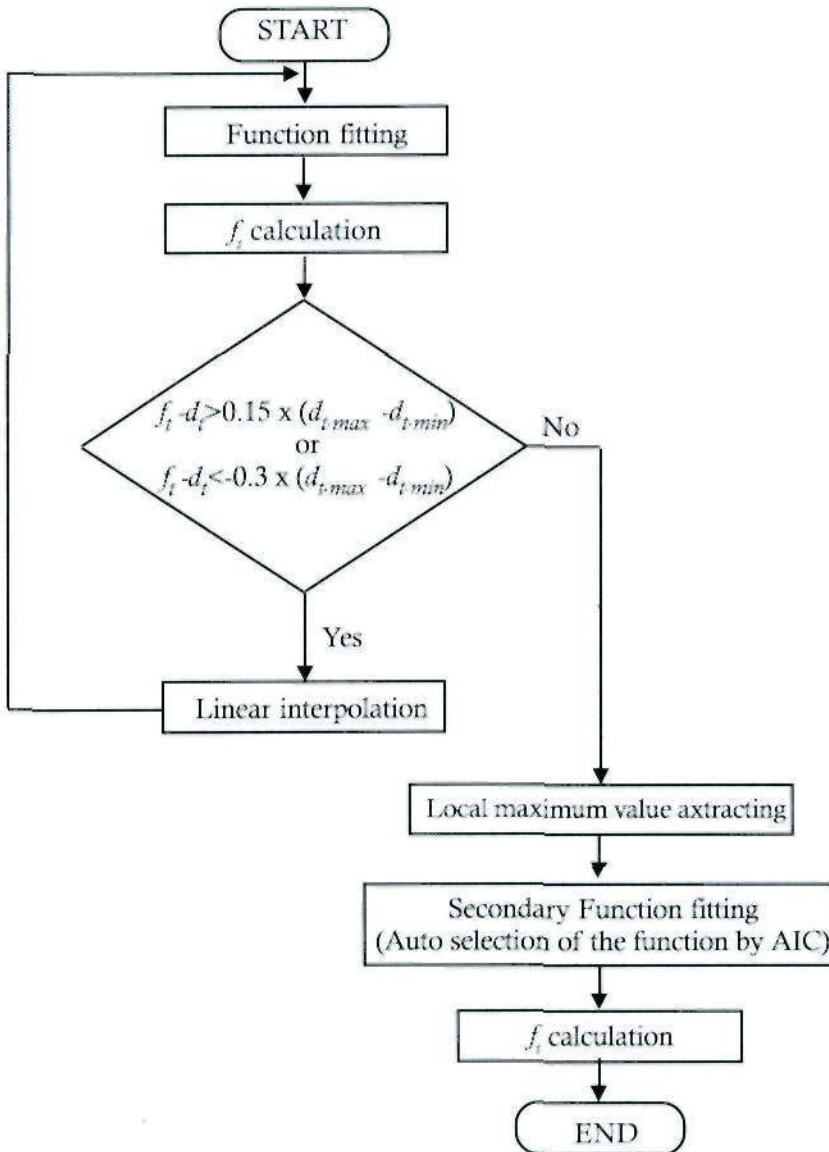


Fig.3 Flowchart of the NRF algorithm.

ous three images that are just after the criterion time image is chosen. And then, the each pixel in the criterion time image is substituted with  $d_i$  that is the smallest value of each maximum value of each group of pixels before and after criterion time.

Akaike's Information Criteria (AIC) (Akaike,1973), a standard for model evaluation, is used (Kitagawa, 1993) for the second fitting of the function.

The result becomes unstable though residual differences from the former data decrease if there are many functions to use for fitting of a time series dataset. The equation to estimate AIC is shown in Equation (3). AIC is calculated from the likelihood logarithm and the number of degree of the model, and a model having minimum AIC value is evaluated as the optimum model. In this study, the optimal coefficients of each function of NRF:  $C_0$ ,  $C_1$ ,  $C_2$  and  $C_{2i}$ , are selected automatically by choosing the minimum AIC value.

$$AIC_j = N\{\log(2\pi\sigma^2) + 1\} + 2(j+1) \quad (3)$$

Where  $N$  is the number of data;  $a^2$  is the estimated value of residual variance; and  $j$  is the number of degree.

### 3.3. Estimating Electric Power Consumption

#### 3.3.1. Problem of Electric Power Consumption Estimated from the OLS-VIS Image

Elvidge used the OLS-VIS data of F 12 to find the distribution of stable lights radiating at night, and the stable nightlight is defined as artificial light from urban area. Moreover, the DN value of each pixel, which the extracted urban area has, is converted into the radiation luminosity with the calibration data before the F12 launch, and relationships between accumulation radiation radiance and the amount of electric power consumption of that city are investigated. Then, there are certain relationships between the accumulation radiation radiance and the amount of electric power consumption, and it is shown that the amount of electric power consumption

could be estimated through this. However, OLS-VIS sensor with a narrow dynamic range has a problem saturated at a high intensity area because of gain and offset control for nighttime observation. And, because all the calibration data before the launch are not publicly available, a conversion to the radiation radiance is difficult with the OLS of F13, F14, and F15. Therefore, this paper attempts to compensate for the DN value using a simple model for the image generated by NRF method. Quality assurance is done in searching for the relationship between the accumulated DN value of urban areas where an NRF image could and estimated electric power consumption. Evaluation of accuracy is done by searching for the relationship between the accumulated DN value of urban areas where extracted by NRF and estimated electric power consumption from the area.

#### 3.3.2. Compensating for Saturation of DN Value Using Deltaic Model

As mentioned above, the DN value of a high radiance zone is saturated in an OLS-VIS image. Therefore, one must correct the amount of electric power consumption in the saturated areas to accurately estimate electric power consumption. The distribution of the radiation radiance is becoming high when it is close to a city center (dense urban areas), but when reaching the outskirts of a city, it is becoming low. So, it assumed that the distribution of the artificial light in urban area became cone-shape, and based on this assumption, the model to correct saturated DN value on this supposition is developed (the Deltaic Model).

The general idea of the Deltaic Model to correct saturation of DN value is shown in Fig.4. The Y-axis shows arbitrary DN value ( $DN_n$ ). The  $DN_{Max}$  shows the maximum of the calculated DN value, and the X-axis shows the total pixel number  $PN_n$  accumulated value contained. Therefore, the number of pixels becomes a large value and the value of X ( $\theta$ ) is expressed as the total number of pixels when the value of Y is can be estimated if the number of pixels of it and from the NRF image is known. When  $\theta$  is computed, the angle

of the right triangle that makes a vertex is calculated by the Equation (4), and the numbers of pixels of arbitrary are calculated by the Equation (5).

$$\tan \theta = \frac{\text{Pixel}_{\text{all}}}{DN_{\text{max}}} \quad (4)$$

$$\text{count}DN_x = \tan \theta (DN_{x+1} - DN_x) \quad (5)$$

Where  $PN_{\text{total}}$  is the total number of pixels in the image; and  $PN_n$  is the number of pixel of  $\text{EW}$ . The images that converted DN value into 239 from 0 in SIDaB are used in this research, and the maximum of DN value is 255 as a result of NRF processing. Therefore, the number of pixels of  $DN_n$  is presumed by calculating the number of pixels of  $DN_g$  and  $DN_{255}$ . The distribution at can be corrected by replacing the result obtained by the Equation (5). This correction is performed for each prefecture, and accuracy is verified by using statistical data of the electric power consumption of each prefecture of Japan.

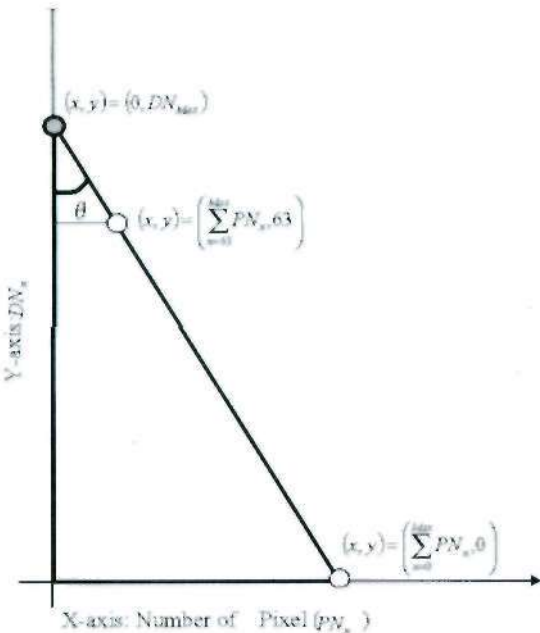


Fig.4. The concept of the Deltaic Model

## IV. Results and Discussion

### 4.1. Urban area Extraction

Fig. 5 shows the area rate of a building lot according to the LUD, a processed image by Elvidge Method and NRF Method. The number of the legend expresses the building lot area in 1 pixel with square meter, and a big number expresses high ratio of the building lot per pixel.

In the Elvidge image, ocean areas are incorrectly classified as dense urban areas through this method, and the areas distant from the city part such as a peninsula that are clearly urban but those area are not classified conversely. This is a possible due to establishing an incorrect threshold value when generating the image (DN value 50 is selected as the threshold). It can be expected to generate the urban area extraction image with high precision by choosing the most suitable threshold. However, one must give careful consideration to the decision of threshold value when using the Elvidge Method.

On the other hand, the area of the high ratio of a building lot is distinguished as an area where a NRF image also emits light. Moreover, the small cities with the low intensity of light that are scattered in a peninsula etc. are also distinguished as a city area. The LUD is overlaid with the NRF image, and it shows that more than a category with the ratio of building area low to the 2nd is corresponded with the city region extracted by NRF. Therefore, the NRF Method can determine artificial nightlight if there is more over 4.3% per unit area of building.

DN value profile in the same section of the Elvidge image and the NRF image are shown in Fig.6. The profile of the Elvidge image is a smooth curve shape. This can be considered that the city boundary region is made indistinct because of diffusion of light including the influence of clouds etc. On the other hand, the DN profile of a NRF image is showing very sharp shape where the point of the DN value changes. Compared to the Elvidge method, it shows the boundary of the city light clearly. There is some area where a calculation exceeded 255 in the urban area with NRF method, but it is dealt with as 255

in this case. The saturation of DN value of OLS-VIS image happens even before the processing, and it becomes the factor of the precision decline in the quantitative analysis. But, there is no problem in the extraction of the urban area.

Furthermore, the Elvidge Method does not detect light that is steady within 0-1 Okm and 30-70km, but the NRF Method as shown in Fig.6, can clearly detect. This is because of arbitrary selection of the threshold in Elvidge method and is an important point to consider when choosing a threshold value. If these are synthesized, Elvidge Method is that the

influence of a city pixel is the remainder in a city circumference region and it shows tendency to reflect higher DN value. Therefore sensitivity to low light declines relatively, and low-density urban areas (i.e., those areas that do not give off much artificial light) are difficult to extract. The NRF Method, on the other hand, not only clearly distinguishes urban boundaries, but it also picks up areas of low artificial light reflectance.

#### 4.2. Estimating Electric Power Consumption

The correlation between the prefectural unit DN mean value and the amount of elec-

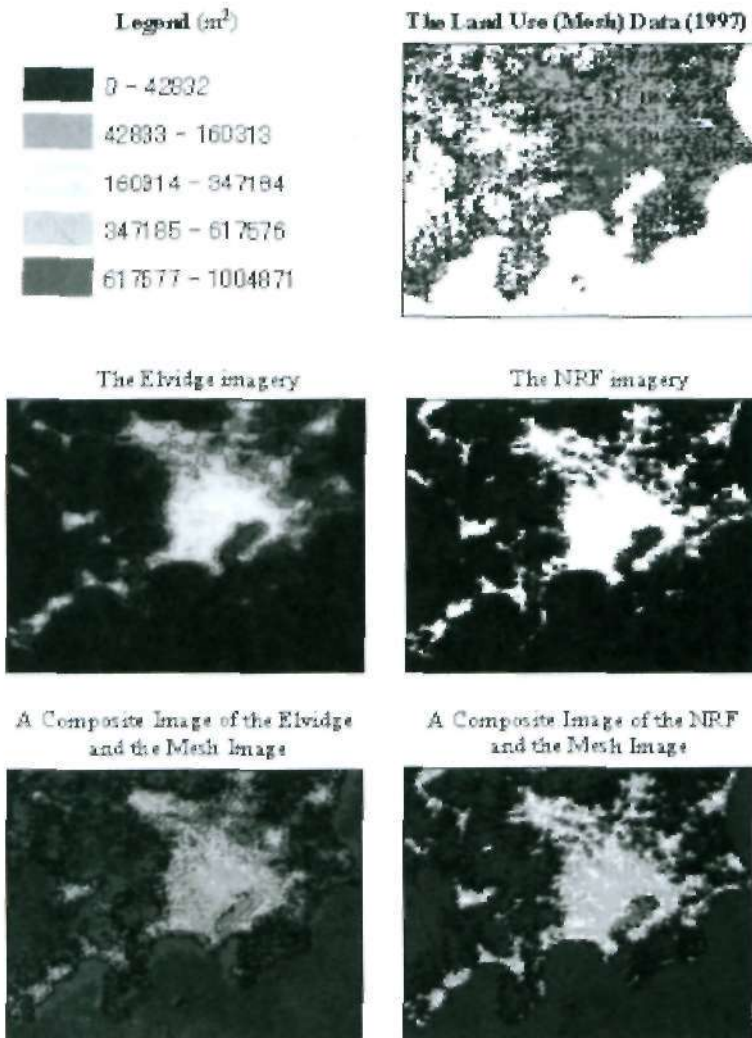


Fig.5. The comparison of an Elvidge image with an NRF image carried out with the basis of the Land Use Data from the Digital National Land Information.

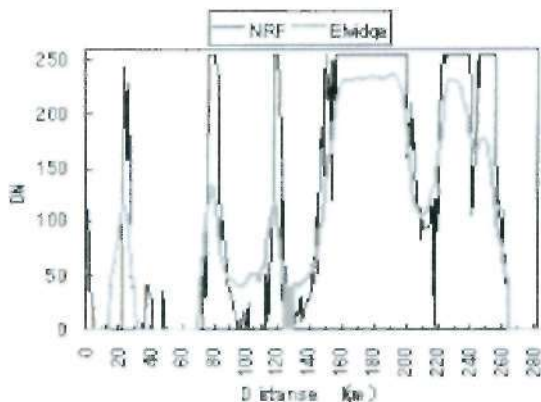
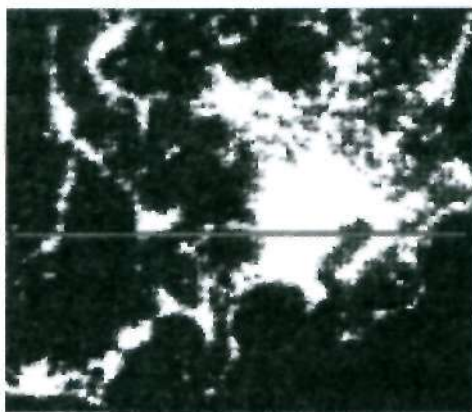


Fig. 6. A profile of the DN value under the cross section line (showing red color) on Kanto area .

trie power consumption is shown in Fig.7. Here, uncorrected data is integrated with DN value of a NRF image per prefecture, and converted it into the value divided by the prefectural number of pixels. Elvidge data is also converted into the value, which processed by the same way as the uncorrected data is processed to the DN value of the Elvidge image. An NRF image is corrected with the Deltaic Model, and the value of DN is compensated.

Comparing the three methods, correlation by the compensation data is the highest with a coefficient of determination ( $R^2=0.725$ ), Elvidge data ( $R^2=0.688$ ) is the second, and correlation by the uncorrected data is the lowest ( $R^2=0.648$ ). Comparing intercepts in case of these regression lines, compensated data is the closest to 0 ( $1E+06$ ), the uncompensated data ( $3E+06$ ) followed the compensated data, and the Elvidge data ( $-4E+06$ ) is the far-

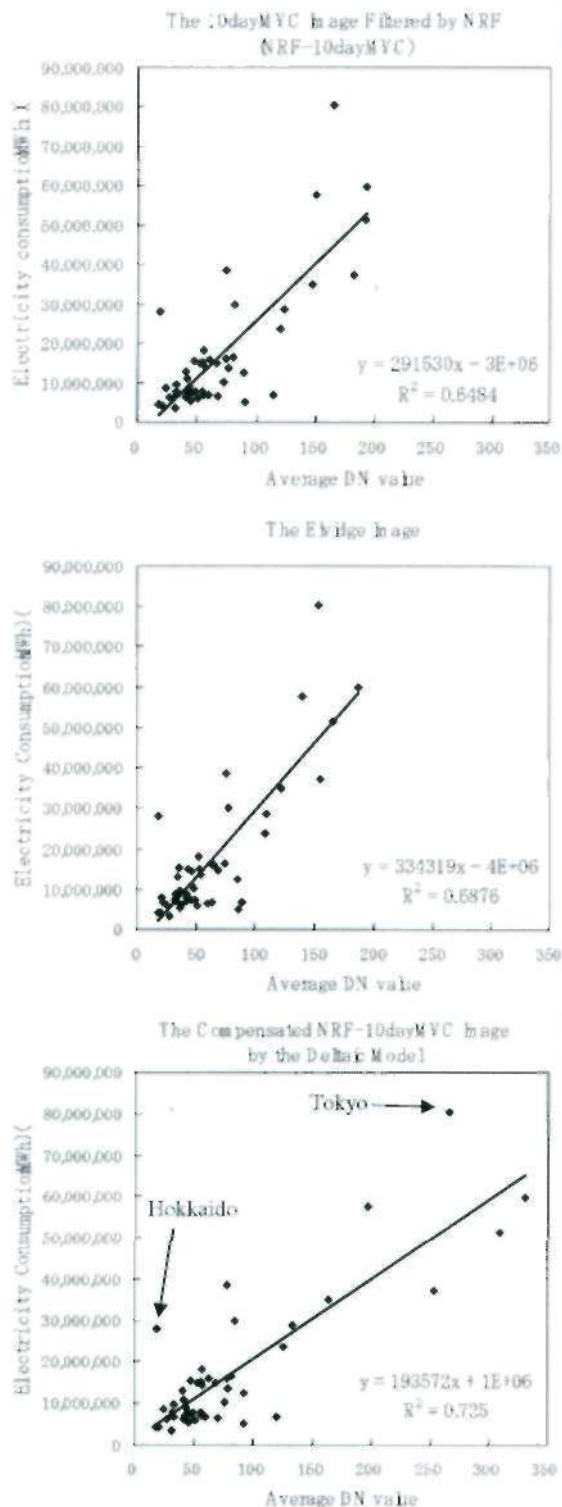


Fig.7. The regression analysis between average DN value and electricity consumption of each prefectures in Japan.

thest from 0. As this cause, the Elvidge method does not count low DN value, and moreover, it is possible that the city circumference area influenced of the strong intensity of light is contained in a city region, and is extracted with slight width in a city region. In other words, Elvidge data becomes low to electric power consumption because lower DN value of the extracted domain is omitted, and the slope is also loose because the range of data distribution is narrow. Opposed that, the sensitivity against the lower light of the compensated data is high, and it is extracted properly in the boundary stage around the urban area. Moreover, the dispersion range of the data is wide, and approximation to the amount of electric power consumption rises.

On the other hand, uncompensated data is that the sensitivity of the lower light and the extraction of a city circumference region is improved than Elvidge data, however it has been processed including the saturation of DN value, so that, the result is showing the middle-result of Compensation data and Elvidge data. This result could say that the consumption electric power could be very accurately estimated by correcting the NRF image with the Deltaic Model.

However, even if compensation is carried out with the deltaic model, there are some data inaccuracies seen in such cases as Tokyo and Hokkaido. This is due to the higher density with saturated DN value of areas such as Tokyo, or the areas of scattered value such as Hokkaido. It is because it compensated collectively in the local unit of a prefecture but not each city area. The improvement of this model, possibly through the idea of regional city unit extraction, will be done in future research.

## V. Conclusion

The method of extracting the artificial stable nightlight distribution from a time series DMSP/OLS-VIS is developed by applying NRF that is developed by authors (2003a, 2003b).

A result by this technique is evaluated by comparing it to imagery derived from the Elvidge Technique (2001) and the LUD.

Through this methodology, the validity of the authors' NRF is proved.

Furthermore, a method to estimate electric power consumption from DMSP/OLS data is developed. A simple model called Deltaic Model is used to estimate values of the artificial nightlight intensity reduced by saturation due to sensor gain, and it tried improvement in accuracy of the amount of electric power consumption estimated lower due to the saturation. The verification of accuracy is determined by using statistical electric power consumption data of each prefecture in Japan, and high correlation ( $=0.725$ ) between the estimated electric power consumption and statistic one is obtained. The average intensity of the artificial stable nightlight can be extracted by using the NRF Method.

It is shown that the parameter of the human activities such as artificial nightlight can be extracted from the OLS-VIS data using the NRF Method, even if the sensor gain is controlled and the condition of observation are not fixed.

## Acknowledgement

The authors are pleased to express their hearty thanks to Dr. Christopher D. Elvidge of National Geophysical Data Center (NGDC) for his kind advice on the characteristics of DMSP/OLS sensors and offer of DMSP/OLS data. The authors would also like to thank Mr. Kazuo Sato and Mr. Toshikazu Morohoshi of National Research Institute for Earth Science and Disaster Prevention for their kind advice and support for using of super computer on the NRF analysis.

DMSP/OLS data have been supplied from NGDC and the agriculture, forestry and fisheries satellite image database system (SIDaB) of the Ministry of Agriculture, Forestry and Fisheries.

## References

- Akaike, H., Information Theory and an Extension of the Maximum Likelihood Principle, 2nd International Symposium on Information Theory, 267-281, 1973.

- Doll, C.N.H., Muller, J. P. and Elvidge, CD., Night-time Imagery as a Tool for Global Mapping of Socioeconomic Parameters and Greenhouse Gas Emissions, *Ambio*, 29(3), 157-162, 2000.
- Elvidge, CD., Baugh, K. E., Kihn, E.A., Kroehl, H.W. and Davis, E.R., Mapping City Lights With Nighttime Data from the DMSP Operational Linescan System. *Photogramm. Eng. Remote Sens.*, 63, 727-734, 1997a.
- Elvidge, CD., Baugh, K. E., Kihn, E.A., Kroehl, H.W, Davis, E.R. and Davis, C, Relation between satellite observed visible-near infrared emissions, Population, and energy consumption., *Int. J. Remote Sens.*, 18, 1373-1379, 1997b.
- Elvidge, CD, Baugh, K. E., Hobson, V.R., Kihn, E.A., Kroehl, H.W, Davis, E.R. and Cocero, D, Satellite inventory of human settlements using nocturnal radiation emissions: a contribution for the global toolchest. *Global Change Biology*, 3, 387-395, 1997c.
- Elvidge, CD., Baugh, K. E., Hobson, V.R., Dietz, J.B., Bland, T., Sutton, P.C and Kroehl, H. W, Radiance Calibration of DMSP-OLS Low-Light Imaging Data of Human Settlements. *REMOTE SENS. ENVIRON*, 68, 77-88, 1999.
- Elvidge, CD, Imhoff, M.L., Baugh, K. E., Hobson, V.R., Nelson, I., Safran.J., Dietz, J.B. and Tuttle, B.T., Night-time light of the world: 1994-1995, *Photogrammetry & Remote Sensing*, 56, 81-99, 2001.
- FEPC, Handbook of Electric Power Industry (in Japanese), by Statistical Committee, The Federation of Electric Power Companies of Japan, Japan Electric Association, Tokyo, 737, 2002.
- Hara, M., Okada, S., Yagi, H., Moriyama, T, Shigehara, K., and Sugimori.Y., Developing and evaluation of the noise reduction filter for the time-series satellite images (in Japanese). *J. The Japan Society of Photogrammetry and Remote Sensing*, 42(5), 2003a.
- Hara, M., Okada, S., Yagi, H., Moriyama, T, Shigehara, K., and Sugimori.Y., Production and evaluation of the cloud free SST time-series using DMSP/OLS Thermal imagery( in Japanese ), *J. Advanced Marine Science and Technology Society*, (in press), 2003b.
- IPCC, Climate Changed, - The IPCC Scientific Assessment —, by J. T. Houghton, G. J. Jenkins and J. J. Ephraums, Cambridge University Press, Cambridge, 339, 1990.
- JMA, Unusual Weather Report '84 (in Japanese), ed. by Japan Meteorological Agency. Printing Bureau, Ministry of Finance, Tokyo, 433, 1984.
- Kitagawa, G, Programming for time series analysis by The FORTRAN77 (in Japanese), Iwanami, Tokyo, 1993.
- Minami, M, ArcMap User's Guide( in Japanese), PASCO Co., Tokyo, 146y2001y
- Nakayama, H. and Tanaka, S, Trend of World Economics using Nighttime Image from the Space (in Japanese), *Chiri (Geography)*, 28(8), 94-103, 1983.
- Nakayama, H., Tanaka, S. and Suga, Y., DMSP Global Nighttime Image and Its Geographical Meaning (in Japanese), *J. The Remote sensing society of Japan*, 13y299-312, 1993.
- Sawada, Y., Development of methodology to reveal seasonal change dynamics of the earth and to evaluate fire spread risk index by using satellite data, (in Japanese), *Asia-Pacific Network for Disaster Mitigation using Earth Observation Satellite*, 34-53y2001
- Sawada, Y., Sawada, H., and Saito, H., Observation of seasonal change dynamics by using high frequency satellite data (in Japanese), *Proceedings of Autumn 2000 Meeting of Advanced Marine Science and Technology Society*, 209-212 , 2000.